Fish and Shellfish Immunology 88 (2019) 150–160

Contents lists available at ScienceDirect

Fish and Shellfish Immunology

journal homepage: www.elsevier.com/locate/fsi

Full length article

LvRas and LvRap are both important for WSSV replication in *Litopenaeus vannamei*

Yi-Ting Tseng[a], Ramya Kumar[a], Han-Ching Wang[a,b,*]

[a] Department of Biotechnology and Bioindustry Sciences, College of Biosciences and Biotechnology, National Cheng Kung University, Tainan, 701, Taiwan
[b] International Center for the Scientific Development of Shrimp Aquaculture, National Cheng Kung University, Tainan, 701, Taiwan

ARTICLE INFO

Keywords:
White spot syndrome virus
Litopenaeus vannamei
WSSV-Induced Warburg effect
LvRas
The mTOR pathway

ABSTRACT

The white Spot Syndrome Virus (WSSV) is a pathogen that causes huge economic losses in the shrimp-farming industry globally. At the WSSV genome replication stage (12 hpi) in WSSV-infected shrimp hemocytes, activation of the PI3K-Akt-mTOR pathway triggers metabolic changes that resemble the Warburg effect. In shrimp, the upstream regulators of this pathway are still unknown, and in the present study, we isolate, characterize and investigate two candidate factors, i.e. the shrimp Ras GTPase isoforms LvRas and LvRap, both of which are upregulated after WSSV infection. dsRNA silencing experiments show that virus replication is significantly reduced when expression of either of these genes is suppressed. Pretreatment with the Ras inhibitor Salirasib further suggests that LvRas, which is a homolog to a commonly overexpressed human oncoprotein, may be involved in regulating the WSSV-induced Warburg effect. We also show that while both the PI3K-Akt-mTOR and Raf-MEK-ERK pathways are activated by WSSV infection, LvRas appears to be involved only in the regulation of the mTOR pathway.

1. Introduction

White spot disease (WSD), which is caused by a large dsDNA virus called the white spot syndrome virus (WSSV), continues to lead to massive economic losses in global shrimp production [1]. WSSV is a relatively complex virus with low sequence homology to other known viruses, and its pathogenesis and virus-host interactions are still not completely understood [2,3]. Recently, using a systems biology approach, we found that WSSV was able to induce metabolic reprogramming at the genome replication stage (12 hpi). In particular, we found that this virus induced aerobic glycolysis (also known as the Warburg effect) as shown by an increase in glucose consumption and lactate secretion [4,5]. The PI3K-Akt-mTORC1 pathway was also implicated as the regulatory pathway that mediated these WSSV-induced shifts in metabolism [4]. However, the question of which upstream factor[s] might control the activation of this pathway has so far not been addressed.

One possible candidate is the small GTPase protein Ras, a human cancer proto-oncogene that has been extensively researched [6]. Activated Ras is known to control not only the PI3K-Akt-mTOR signaling pathway [7–10] but also the Raf-MEK-ERK pathway [11–13]. Further, active Ras isoforms have been reported to affect cell metabolisms, especially the enhancement of glycolytic flux and lactate production [14–16]. In most cancer cells, by triggering both of the above pathways, oncogenic, constitutively active Kras promotes aerobic glycolysis, glutaminolysis and other metabolic reprogramming [6,12,17–22]. Ras activation plays a similar role during human adenovirus type 36 (Ad-36) infection, where it leads to an increase in the PI3K pathway-dependent uptake of glucose [23].

Ras proteins are members of the Ras subfamily, which, together with five other subfamilies (Ral, Rap, Rheb, Rad and Rit) [24,25] belongs to the Ras family. The Ras family and four other main families (Rho, Rab, Ran and Arf/Sar) [26] in turn belong to the Ras superfamily. All of the eukaryotic, small GTP-binding proteins (G proteins, or small GTPase proteins) belong either to the Ras superfamily or to one of several other superfamilies. These proteins are involved in the regulation of various cellular mechanisms, including cytoskeleton remodeling, cell growth, proliferation and differentiation [27,28]. All of them can be activated by replacing GDP with GTP, and inactivated by hydrolyzing GTP to GDP [29,30]. When activated, i.e. when bound to GTP, proteins in the Ras superfamily facilitate binding with effectors and thereby initiate signaling cascades [11,31]. In all of these proteins, GTP hydrolysis and effector protein interactions are mediated by the Ras domain. This domain consists of 5 conserved G box GDP/GTP-

* Corresponding author. Department of Biotechnology and Bioindustry Sciences, College of Biosciences and Biotechnology, National Cheng Kung University, Tainan, 701, Taiwan.
E-mail address: wanghc@mail.ncku.edu.tw (H.-C. Wang).

https://doi.org/10.1016/j.fsi.2019.02.035
Received 2 October 2018; Received in revised form 13 February 2019; Accepted 15 February 2019
Available online 19 February 2019

binding motif elements, G1–G5, which are highly evolutionarily conserved. In most organisms, proteins in the Ras superfamily also include hypervariable regions (HVRs) in the C-terminal [32,33]. Following the HVR, proteins in the Ras and Rho families have a terminal CaaX motif. This motif is responsible for the initiation of post-translational lipid modification (i.e. farnesylation), which results in re-localization to the plasma membrane and is an essential step in Ras activation [34–39].

In the present study, we identified, isolated and characterized white shrimp genes for both Ras and Rap, and we investigated the involvement of Ras in the WSSV-induced Warburg effect. We also investigated the possible involvement of the PI3K-Akt-mTOR and Raf-MEK-ERK pathways in mediating the observed Ras-dependent metabolic changes.

2. Materials and methods

2.1. Experimental animals

In this study, white shrimp (*Litopenaeus vannamei*; mean weight: 2–3 g) were obtained from the International Center for the Scientific Development of Shrimp Aquaculture, National Cheng Kung University (NCKU) and from the Department of Aquaculture, National Pingtung University of Science and Technology (NPUST). Upon arrival, in order to reduce any stress induced by transportation, the shrimp were transferred to a water tank system containing sterilized seawater (30 ppt at 25–27 °C) for at least 1 day (no more than 3 days).

2.2. Cloning of full-length cDNAs of LvRas and LvRap

An in-house *L. vannamei* stomach transcriptomic database [40] was used to search for homologs of the human Ras isoform Kras (NCBI Accession number: NP_004976.2). Two contigs, Lv23558.1 and Lv153409.1, were found to show high homology with human Kras, and these were used to design primer sets to amplify these two genes from white shrimp hemocytes cDNA (Table 1). The resulting PCR amplicons were cloned in T&A Vector (RBS Biosciences) and sequenced. The Basic Local Alignment Search Tool (BLAST) identified the first sequence as orthologous to Ras, and the second sequence as orthologous to Ras-like GTPase Rap, which is a member of the Ras family of GTPases. We named these orthologs LvRas and LvRap, respectively, and the corresponding sequences have been uploaded to NCBI with accession numbers MK392631 and MK392632. The full-length amino acid sequences of LvRas and LvRap were aligned with other selected Ras GTPases from the GenBank database by using the GeneDoc program and Cluster Omega software.

2.3. Virus and virus inoculum

The Taiwan isolate of the white spot syndrome virus (WSSV) (GenBank Accession no. AF440570) was used in this study. The stock of WSSV inoculum (3.3×10^4 WSSV copies/μl) was prepared from WSSV-infected moribund white shrimp as described previously [3,4] and stored at −80 °C. For the challenge experiments, the experimental WSSV inoculum was prepared from the WSSV stock by dilution (10^{-4}) with phosphate buffer saline (PBS) (137 mM NaCl, 2.7 mM KCl, 10 mM Na_2HPO_4, 2 mM KH_2PO_4). Shrimp were challenged with WSSV inoculum (100 μl/shrimp) by intramuscular injection. The WSSV challenge dosage used in this study resulted in an approximately 50% WSSV-induced mortality rate at 3 days post challenge. Shrimp injected with PBS were used as controls. At each time point (12 and 24 hpi), 4 pooled hemocytes, pleopod and gill samples were collected (3 shrimp per sample) from each group. As described below, hemocytes samples were subjected to real-time PCR to measure the mRNA levels of host genes and WSSV genes, while the pleopod samples were used to quantify the number of WSSV genomic DNA copies as described in Su [4]. The pooled gill samples were subjected to western blotting to determine protein expression levels [4].

Table 1
Primers used in this study.

Gene	Primer	Primer sequence (5' — 3')	Usage
LvRas			
	LvRas-F	ATGACGGAATACAAGCTCGTCG	PCR
	LvRas-R	CTAGAACACAATGCACTTCCTC	PCR
	LvRas-qF	ATGGTTTTGGTGGGCAACA	Real-time PCR
	LvRas-qR	GCCTGCTGCATGTCCATTG	Real-time PCR
	T7-LvRas-F	*TAATACGACTCACTATAGGGAGAATGACGGAATACAAGCTCGTCG	dsRNA synthesis
	T7-LvRas-R	*TAATACGACTCACTATAGGGAGACTAGAACACAATGCACTTCCTC	dsRNA synthesis
LvRap			
	LvRap-F	ATGCGTGAATACAAGATTGTGG	PCR
	LvRap-R	TTATAAAAGGCAACACTTCTTC	PCR
	LvRap-qF	TAAGATCAATGTCAATGACAT	Real-time PCR
	LvRap-qR	ATTTAACTTTCTGTCGGGGG	Real-time PCR
	T7-LvRap-F	*TAATACGACTCACTATAGGGAGAATGCGTGAATACAAGATTGTGG	dsRNA synthesis
	T7-LvRap-R	*TAATACGACTCACTATAGGGAGATTATAAAAGGCAACACTTCTTC	dsRNA synthesis
Firely-Luciferase			
	Luc-F	GTTCAGCGTGTCCGGCGAG	PCR
	Luc-R	GTTCTTCTGCTTGTCGGCC	PCR
	T7-Luc-F	*TAATACGACTCACTATAGGGAGAGTTCAGCGTGTCCGGCGAG	dsRNA synthesis
	T7-Luc-R	*TAATACGACTCACTATAGGGAGAGTTCTTCTGCTTGTCGGCC	dsRNA synthesis
EF1-α			
	EF1α-F	ATGGTTGTCAACTTTGCCC	RT-PCR
	EF1α-R	TTGACCTCCTTGATCACACC	RT-PCR
	EF1α-real-F	ACGTGTCCGTGAAGGATCTGAA	dsRNA synthesis
	EF1α-real-R	TCCTTGGCAGGGTCGTTCTT	dsRNA synthesis
WSSV VP28			
	VP28-real-F	AGTTGGCACCTTTGTGTGTGGTA	Real-time PCR
	VP28-real-R	TTTCCACCGGCGGTAGCT-	Real-time PCR
Others			
	Anchor-dTv	GACCACGCGTATCGATGTCGACTTTTTTTTTTTTTTTV	cDNA synthesis

* The added T7 promoter sequence is underlined.

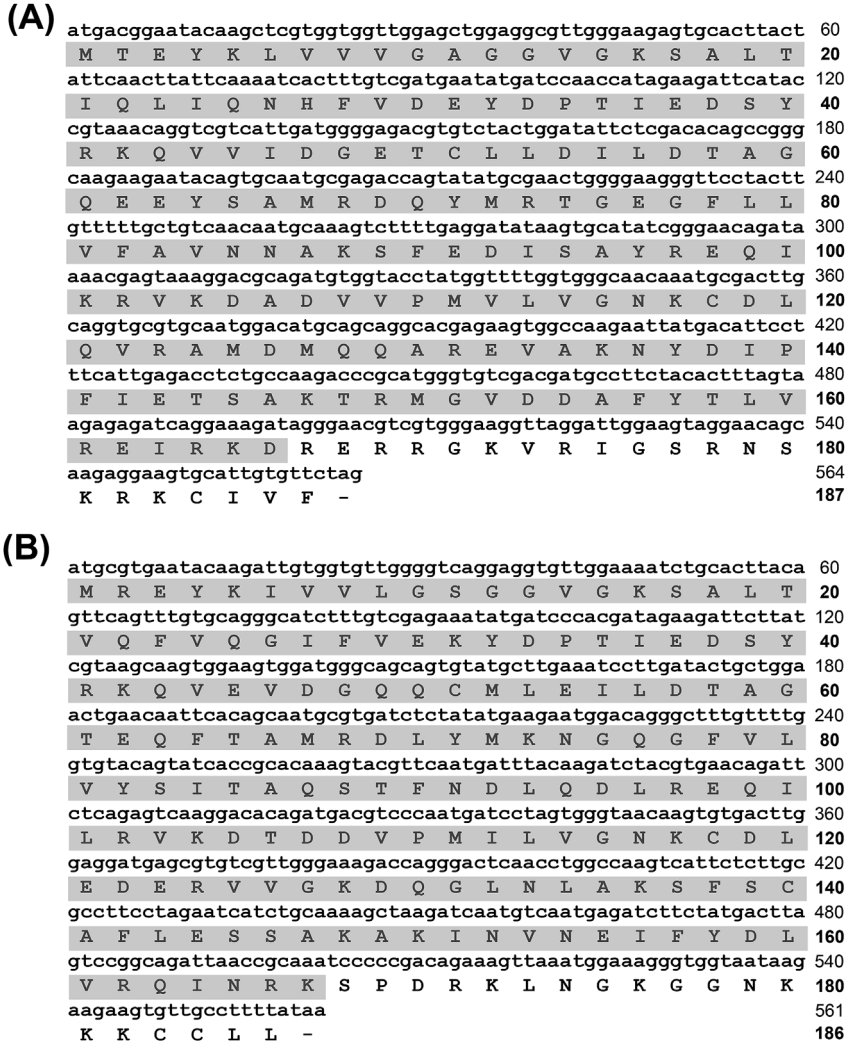

Fig. 1. Nucleotide and deduced amino acid sequences of (A) LvRas and (B) LvRap. The deduced amino acid sequences of LvRas and LvRap are shown under the corresponding nucleotide sequences. The Ras domains in LvRas and LvRap are shaded.

2.4. Quantification of host genes and the WSSV structural gene VP28 by real-time PCR

Total RNA was extracted from the pooled shrimp hemocytes sample and mixed with Superscriptase II Reverse Transcriptase (Invitrogen) and Anchor-dTv primer (Table 1) to synthesize the cDNAs. To measure the relative expression levels of the host genes (LvRas, LvRap and an internal control gene EF1α) and WSSV VP28, cDNAs were subjected to real-time PCR using the Bio-Rad detection system with KAPA SYBR® FAST Master Mix (KAPA). Primer sets used for real-time PCR are listed in Table 1. Data values of all samples were calculated by the $2^{-\Delta\Delta CT}$ method and normalized relative to the housekeeping gene EF1α. After the Empirical Rule was performed on all data for the detection and exclusion of statistical outliers, statistically significant differences between groups were analyzed either by Student's t-test or Tukey's test for comparing multiple treatments.

2.5. Quantification of the WSSV genome copy number

Genomic DNA was extracted from pooled pleopod samples using a DTAB/CTAB DNA extraction kit (GeneReach Biotechnology Corp.). WSSV viral genome copy numbers were measured using the IQ Real™ WSSV quantitative system (GeneReach Biotechnology Corp.). Statistical analysis was performed as described before.

2.6. Measurement of Ras activation

The Ras-GTP levels were determined by using a Ras activation assay kit (Cell Biolabs, Inc.). For this assay, to ensure a good yield and quality of proteins, lysates were extracted from shrimp gill tissue instead of hemocytes. Samples of gill tissue were lysed by homogenization in ice-cold 1x Assay/Lysis buffer with protease inhibitor cocktail and phosphatase inhibitor (Roche), and protein concentrations were determined using the Bradford Protein Assay (Bio-Rad). For the total Ras and beta-actin input control, lysates containing 25 μg of protein were mixed with SDS-sample buffer and subjected to western blotting as described below. For the active Ras-GTP pull-down assay, lysates containing approximately 2.5 mg of protein were collected into new tubes, the volume was adjusted to 1 ml with ice-cold 1x Assay/Lysis buffer, 40 μl Raf1 RBD Agarose bead slurry was added, and the mixture was incubated at 4 °C for 1 h. After centrifugation, the Raf1 RBD Agarose beads were washed three times with ice-cold 1x Assay/Lysis buffer. The activated Ras that was bound to these beads was then dissolved in SDS-sample buffer and subjected to western blotting with Ras antibody. For the positive and negative controls, lysates containing ~2.5 mg of protein extracted from healthy, untreated shrimp were collected, adjusted to a volume of 1 ml with ice-cold 1x Assay/Lysis buffer and 20 μl of 0.5 M EDTA was added. 10 μl of GTPγS was added to the positive control while 10 μl of GDP was added to the negative control. After incubation at 4 °C for 1 h, 65 μl of 1M $MgCl_2$ was added to stop the

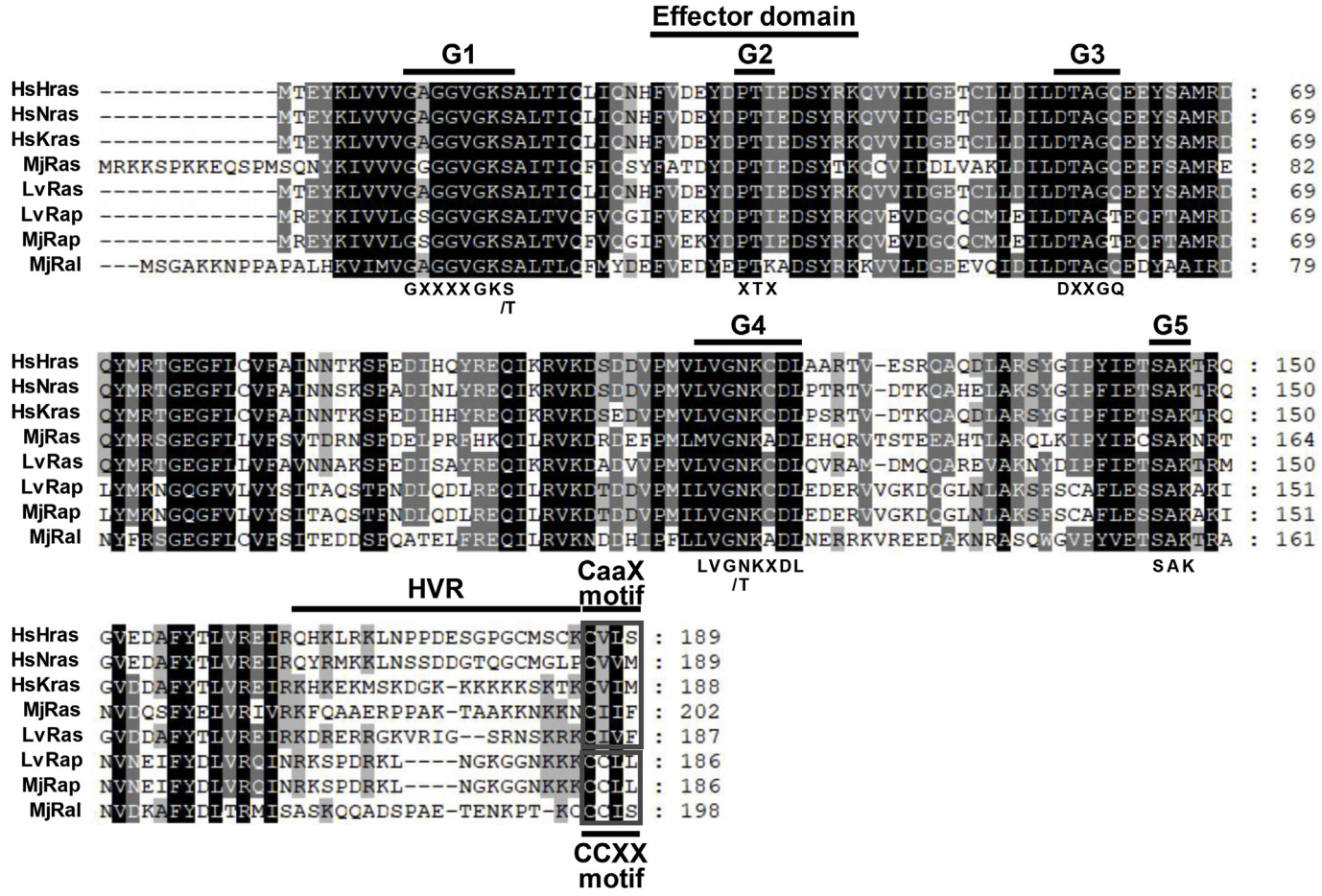

Fig. 2. Multiple alignment of deduced amino acid sequences for LvRas, LvRap, three Ras superfamily members from kuruma shrimp and three human Ras isoforms. The conserved G1 ~ G5 motifs, core effector region, hypervariable region (HVR) and the CaaX/CCXX motifs are indicated. NCBI accession number: human Hras [CAG38816], human Nras [AAA60255], human Kras [XP_011518955], kuruma prawn Ras [ANR94954.1], kuruma prawn Rap [ANR94953.1], kuruma prawn Ral [ANR94955.1].

reaction. Aliquots of the positive and negative control lysates containing 2.5 mg of protein were then subjected to the pull-down assay and western blotting as described above; portions of the positive and negative control lysate containing 25 μg of protein were subjected only to western blotting.

2.7. Western blotting

In addition to the Ras activation samples described above, western blotting was also performed on pooled gill samples (3 shrimp/sample) that were collected and immediately stored in liquid nitrogen before use. These samples were homogenized in 0.33x PBS with protease inhibitor and phosphatase inhibitor (Roche), subjected to the Bradford Protein Assay (Bio-Rad) to determine protein concentrations, and portions of lysate containing ~100 μg of protein were prepared. All samples for western blotting were then mixed with SDS-sample buffer (1% SDS, 15% glycerol, 10 mM Tris-HCl [pH 6.8], 10% beta-mercaptoethanol) to a final volume of 40 μl, and then separated by 15% SDS-PAGE (sodium dodecyl sulfate polyacrylamide gel electrophoresis). After transfer onto polyvinylidene fluoride (PVDF) membranes and blocking with 0.5% BSA in TBST [0.5% Tween 20, 200 mM NaCl, 50 mM Tris-HCl, pH7.5] for 10.5 h at 4 °C, the membranes were incubated with the respective primary antibodies in TBST at 4 °C. Following several extensive washes with TBST, membranes were then incubated in TBST containing horseradish peroxidase (HRP) conjugated goat anti-mouse secondary antibody (Santa Cruz), or HRP conjugated goat anti-rabbit secondary antibody (Invitrogen) for 1 h at room temperature. After further washing with TBST several times, the signals were developed by ECL detection agents (PerkinElmer). The ImageQuant™ LAS 4000 chemiluminescence system was used for signal detection. Intensities of specific protein bands were determined and quantified using ImageJ software.

2.8. Antibodies

The primary antibodies used in this study were: Ras Antibody (Cell signaling; Catalog No. 3965) for detecting Ras; p44/42 MAPK (Erk1/2) (137F5) Rabbit mAb (Cell signaling; Catalog No. 4695) for detecting total ERK protein; Phospho-p44/42 MAPK (Erk1/2) (Thr202/Tyr204) (D13.14.4E) XP® Rabbit mAb (Cell signaling; Catalog No. 4370) for detecting phospho-ERK (which is used to indicate activation of the Raf-MEK-ERK pathway); Phospho-4E-BP1 (Thr37/46) (236B4) Rabbit mAb (Cell signaling; Catalog No. 2855) for detecting phospho-4E-BP1(which is used to indicate activation of the PI3K-Akt-mTOR pathway); and Beta-actin antibody (Millipore; Catalog No. # MAB1501) for the internal control. In-house antibodies that recognize the WSSV structural protein VP28 and the major WSSV non-structural protein ICP11 were prepared as described previously [41].

2.9. The in vitro synthesis of LvRas and LvRap dsRNA

To produce the linear DNA templates, partial cDNA fragments of LvRas, LvRap and luciferase with lengths of approximately 500–600 bp were amplified by RT-PCR with the primer sets LvRas-F/LvRas-R,

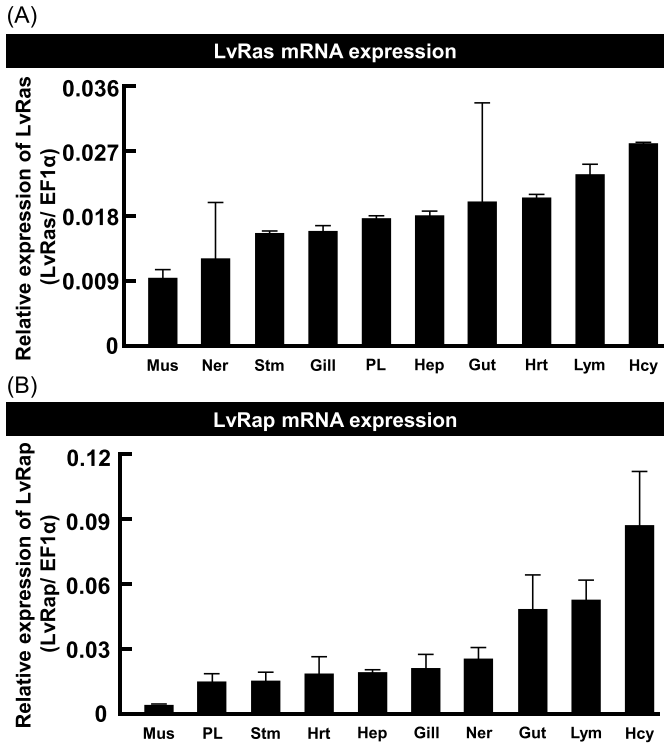

Fig. 3. Real-time qPCR results for (A) LvRas and (B) LvRap mRNA expression in 10 shrimp tissues. Samples from hemocytes (Hcy), pleopod (Pl), gill, heart (Hrt), hepatopancreas (Hep), intestine (Ins), nervous tissue (Ner), muscle (Mus), stomach (Stm) and lymphoid organ (Lym) were amplified using gene specific primer sets (Table 1). The $2^{-(\Delta\Delta Ct)}$ method was used to calculate relative gene expression.

LvRap-F/LvRap-R and Luc-F/Luc-R (Table 1). The T7 promoter sequence was fused onto both strands of these linearized DNA templates using PCR with the following specific primer sets: T7-LvRas-F/LvRas-R, LvRas-F/T7-LvRas-R; T7-LvRap-F/LvRap–R; LvRap-F/T7-LvRap-R; T7-Luc-F/Luc-R and Luc-F/T7-Luc-R (Table 1). The resulting amplicons were then used as templates to synthesize ssRNAs using the T7 RiboMAX Express large-scale RNA production system (Promega) according to the manufacturer's instructions. dsRNAs were produced by mixing the corresponding ssRNAs together, annealing at 70 °C and cooling down to room temperature. The dsRNAs were purified using phenol/chloroform/isoamyl alcohol extraction, verified by agarose gel electrophoresis, and quantified by using a UV spectrophotometer. The dsRNAs were stored at −80 °C before use.

2.10. dsRNA silencing

For the dsRNA-mediated gene silencing experiments, shrimp in the experimental groups were injected intramuscularly with LvRas dsRNA or LvRap dsRNA at 1 μg dsRNA per g shrimp body weight, while shrimp in the control groups were injected intramuscularly with PBS only or Luc dsRNA. Three days after the dsRNA treatment, shrimp were injected with WSSV or with the PBS vehicle only. At 3 days post dsRNA treatment and 24 h post WSSV injection, pooled hemocytes samples (3 shrimp in each pool sample) were collected from each group and used to determine both the efficiency of the gene silencing and the mRNA expression level of the WSSV structural gene VP28. At 24 h post WSSV injection, pooled pleopod samples (3 shrimp in each pool sample) were also collected and used to measure the WSSV genome copy number as described above.

2.11. Preparation of the Ras inhibitor Salirasib and confirmation of the effect of Salirasib on LvRas activation

Salirasib powder (farnesylthiosalicylic acid [FTA], Sigma-Aldrich Co.) was dissolved in 99% ethanol to produce the stock Salirasib solution. This stock was then diluted with PBS (pH8.0) to produce different concentrations of the final working Salirasib solution in 0.3% ethanol. Two hours before WSSV injection, shrimp were injected intramuscularly with 100 μl of the working Salirasib solution at 10–35 μg/g shrimp body weight. Shrimp treated with 100 μl of the vehicle only (ie. 0.3% ethanol) were used as controls. Pooled samples were collected, and mRNA expression levels and WSSV copy numbers were determined as described above. To confirm the effect of Salirasib on LvRas GTPase activity, shrimp were treated with the highest dosage of Salirasib (35 μg/g shrimp body weight) followed by WSSV challenge. At 24 hpi, pooled gill samples (6 shrimp per sample) were collected and Ras activation was measured as described above.

2.12. Effect of treatment with Ras inhibitor Salirasib on the concentration of glucose and lactate in hemolymph

After pretreatment with Salirasib or the 0.3% ethanol vehicle only, shrimp were injected with WSSV or PBS, and at 12 and 24 h post challenge, pooled hemolymph samples (3 shrimp/sample) were collected without anticoagulant from each group. After being kept at 4 °C for 12–16 h, the samples were then centrifuged (800 × *g* for 10 min), and the supernatants were transferred into new tubes. The concentrations of glucose and lactate in the supernatants were measured by using Glucose GLUC-PAP (Randox Laboratories Ltd.) and Lactate (Fortress Diagnostics, Ltd.).

3. Results

3.1. Both LvRas and LvRap were found in our L.vannamei transcriptomic database

A search for the human Kras sequence (NCBI Accession number: NP_004976.2) against our in-house *L.vannamei* transcriptomic database found two contigs (Lv23558.1 and Lv153409.1) with high homology. Primer sets corresponding to Lv23558.1 and Lv153409.1 were designed to confirm the cDNA sequences of these two genes by using gene cloning (Table 1). The resulting sequences were checked against the NCBI database and identified by BLAST as a Ras protein and a Ras-like protein (Rap). We named these proteins LvRas and LvRap respectively. As Fig. 1 shows, LvRas consists of 564 bp encoding 187 amino acid residues with a molecular weight of approximately 21.33 kDa, while LvRap consists of 561 bp encoding 186 amino acid residues with a molecular weight of approximately 20.89 kDa. A SMART search revealed that LvRas and LvRap both have a Ras domain (residues 1–166 in LvRas [Fig. 1A] and residues 1–167 in LvRap [Fig. 1B]). The GeneDoc program revealed that LvRas was similar to LvRap with 50% identity and 71% similarity.

Fig. 2 shows the amino acid sequence alignment of LvRas, LvRap, three members of the Ras superfamily from kuruma shrimp *Marsupenaeus japonicas* (MjRas, MjRap and MjRal), and three human Ras isoforms (Hras, Nras and Kras). The typical guanine nucleotide binding domains (G1– G5) were found in all the listed Ras proteins, and LvRas contained the corresponding conserved sequences GX(4)GKS/T, YDPTIEDSY, DXXGQ, LVGNKXDL and SAK in all five of these domains as well as the conserved core effector sequence FVDEYDPTIEDSYRK around the threonine35 in the G2 domain. LvRap, on the other hand, did not match the consensus sequence for G3 or for the core effector region. More importantly, the C-terminal CaaX motif, which is involved in the membrane localization of Ras, was also found in LvRas, whereas the same region in LvRap conformed to a conserved sequence (CCXX) that is only found in other members (Rap, Rho, and Rab) of the Ras

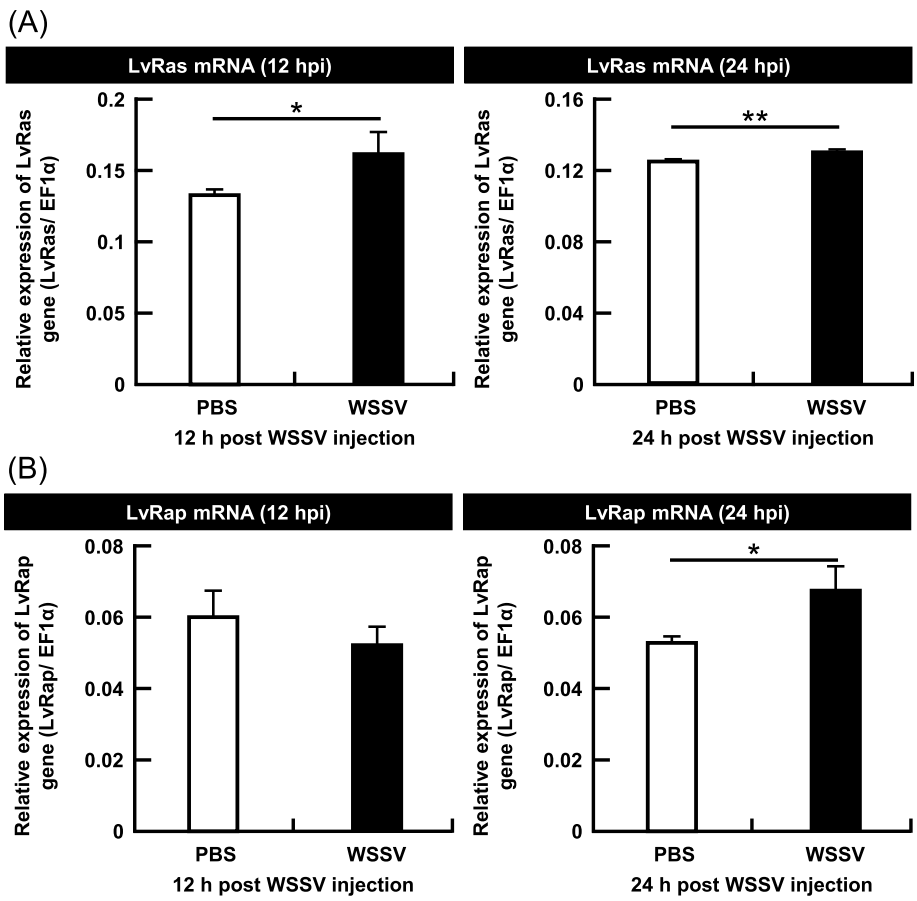

Fig. 4. mRNA expression of LvRas and LvRap in shrimp hemocytes during WSSV infection. Real-time PCR was used to measure the gene expression levels of (A) LvRas and (B) LvRap in pooled hemocytes samples collected from WSSV-infected shrimp at 12 and 24 hpi. Asterisks indicate a significant difference between the target mRNA levels and those in the corresponding PBS control (*p < 0.05, **p < 0.01).

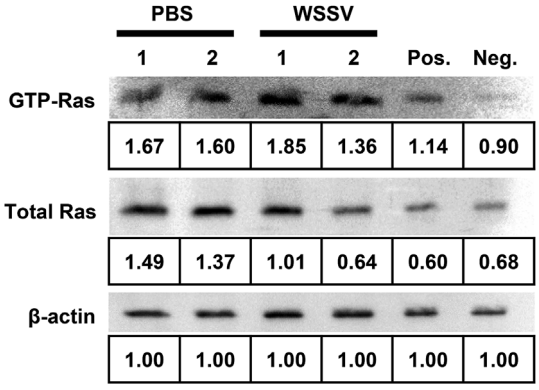

Fig. 5. Pull-down assay for activated Ras in shrimp gills at the late stage of WSSV infection. At 24 h post WSSV injection, 2 pooled gill samples (3 shrimp in each pool) were collected and total protein lysates were extracted. A portion (2.5 mg protein) of the extracted lysates was subjected to a GTP-Ras pull-down assay with Raf-RBD beads, and activated Ras was then detected by western blotting with a Ras antibody. Another portion (25 μg protein) of the extracted lysates was subjected directly to western blotting with the same Ras antibody and with an antibody for β-actin for use as a normalizing control. Total gill protein lysates from untreated shrimp were used for the positive and negative controls by adding GTPγS to activate endogenous Ras, and by adding GDP to inactivate the endogenous Ras, respectively. After quantifying the bands by using the ImageJ Gel Analysis program, the intensities of each protein band were normalized against the β-actin internal control.

superfamily. Based on the sequence homology of the flexible C-terminal hypervariable regions (HVRs), LvRas and LvRap show no obvious resemblance to any of the other Ras isoforms.

3.2. The mRNA levels of LvRas and LvRap were increased during WSSV infection

Tissue tropism patterns suggest that LvRas and LvRap were highly expressed in hemocytes (Hcy) and the lymphoid organ (Lym) (Fig. 3). Expression levels were lowest in the muscle (Mus).

To elucidate if WSSV infection affects LvRas expression, we measured changes in LvRas mRNA levels after WSSV challenge. In the hemocytes collected from WSSV-infected shrimp, at 12 hpi (the WSSV genome replication stage) only LvRas mRNA was significantly upregulated (by a factor of 1.22), while at 24 hpi (the late stage), the mRNAs of LvRas and LvRap were both significantly induced (by a factor of 1.04 and 1.28, respectively; Fig. 4).

3.3. Both LvRas and ERK showed increased activation during WSSV infection

To investigate LvRas activation after WSSV infection, protein lysates from WSSV-infected gills were incubated with GST-Raf-1 RBD agarose beads in order to pull down the GTP-bound form of LvRas. The LvRas activity was determined by the ratio of GTP-Ras to total Ras, and the mean value of this ratio was found to be 1.73 times higher in the WSSV group (Fig. 5).

We next used western blotting to confirm the protein level of Ras and one of its downstream factors, ERK, in pooled shrimp samples collected from shrimp at 24 hpi. As Fig. 6 shows, the protein level of LvRas was elevated at 24 hpi compared to the PBS controls (approximately 2.04 fold greater; Fig. 6). In addition, WSSV infection resulted in increased levels of phosphorylated ERK (pERK) (2.36 fold greater) and total ERK (1.58 fold greater) (Fig. 6).

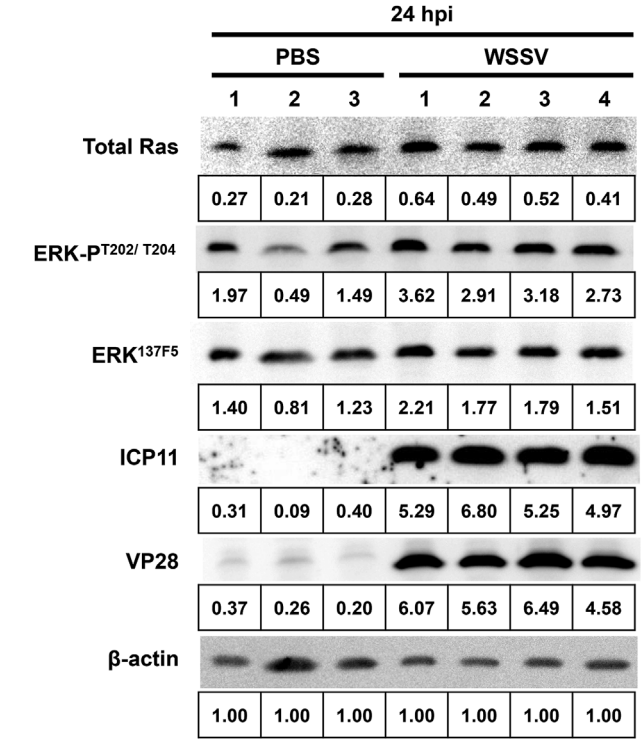

Fig. 6. Protein expression of Ras, pERK and ERK in shrimp gills at the late stage of WSSV infection. At 24 h post WSSV injection, 3 or 4 pooled gill samples (3 shrimp in each pool) were collected and total protein lysates were extracted. Western blotting was then performed with the following antibodies: Ras antibody; phospho-p44/42 MAPK (Erk1/2) (Thr202/Tyr204); and p44/42 MAPK (Erk1/2) (137F5). Two WSSV viral proteins (ICP11 and VP28) were used as proxies to indicate the WSSV infection state. After quantifying the bands by using the ImageJ Gel Analysis program, the intensities of each protein band were normalized against a β-actin internal control.

3.4. *In vivo knockdown by RNA interference suggests that LvRas and LvRap are both important for WSSV replication*

To further investigate the importance of both LvRas and LvRap for WSSV replication, we used *in vivo* dsRNA-mediated gene silencing to suppress the mRNAs of LvRas and LvRap by injecting the corresponding dsRNA into shrimp. Shrimp treated with a non-specific dsRNA, Luc RNA, were used as the non-specific dsRNA injection group. When samples from each of the three experimental groups were collected 3 days after injection, both LvRas and LvRap mRNA were found to be specifically and significantly decreased by their respective dsRNAs (Fig. 7).

The remaining shrimps from the same experimental groups were further challenged with WSSV, and specific gene silencing was still observed at 24 hpi after this challenge (Fig. 8A and B). In the groups of shrimp injected with LvRas dsRNA and LvRap dsRNA, the WSSV VP28 mRNA expression in hemocytes was significantly reduced compared to the Luc dsRNA-treated group, while no significant difference was observed between the LvRas dsRNA- and LvRap dsRNA-treated groups (Fig. 8C). Similar results were found for the number of WSSV genome copies in pleopod samples taken from the same shrimp (Fig. 8D).

3.5. *In vivo suppression of LvRas with the inhibitor Salirasib further suggests its involvement in WSSV replication*

To further confirm the role of LvRas in regulating WSSV replication, at 2 h before shrimp were challenged with WSSV, we pre-treated shrimp with Salirasib (also called Farnesylthiosalicylic acid [FTS]), which inhibits Ras activity by disrupting the translocation of Ras to the plasma membrane [42]. At 24 h post WSSV injection, the highest concentration of Salirasib (35 μg/g shrimp) significantly reduced both the WSSV genome copy number and the expression level of WSSV VP28 mRNA (Fig. 9A and B). At 24 h post WSSV injection, pretreatment with this same high dosage also resulted in the lowest level of LvRas GTPase activity (Fig. 9C). Taken together these results suggest that LvRas activation is important for WSSV replication.

3.6. *LvRas activation is critical for the WSSV-induced Warburg effect*

To investigate whether LvRas activation is involved in triggering the WSSV-induced Warburg effect, we pre-treated shrimp with Salirasib (35 μg/g shrimp) to suppress LvRas activation before injection with WSSV. We then monitored changes in glucose and lactate, which are two characteristic hallmarks of the Warburg effect [43–47].

At 12 hpi (the WSSV genome replication stage), the PBS control groups showed no difference in serum glucose levels. By contrast, after WSSV challenge, there was a significant reduction in glucose levels in both the ethanol and Ras-inhibitor groups (Fig. 10a). At the same time, lactate levels in the serum were significantly elevated in the two control groups (i.e. the PBS group and the vehicle-treated group). By contrast, after the LvRas was suppressed by the Salirasib treatment, no significant accumulation of lactate in hemolymph was observed (Fig. 10A). No Warburg effect for either glucose or lactate was observed at 24 hpi in any of the three groups (Fig. 10B).

3.7. *LvRas activation activates the PI3K-mTOR pathway, but not the ERK pathway*

In humans, Ras is known to regulate two pathways involved in the Warburg effect, i.e. Raf-MEK-ERK and PI3K-Akt-mTOR [48,49]. Fig. 6

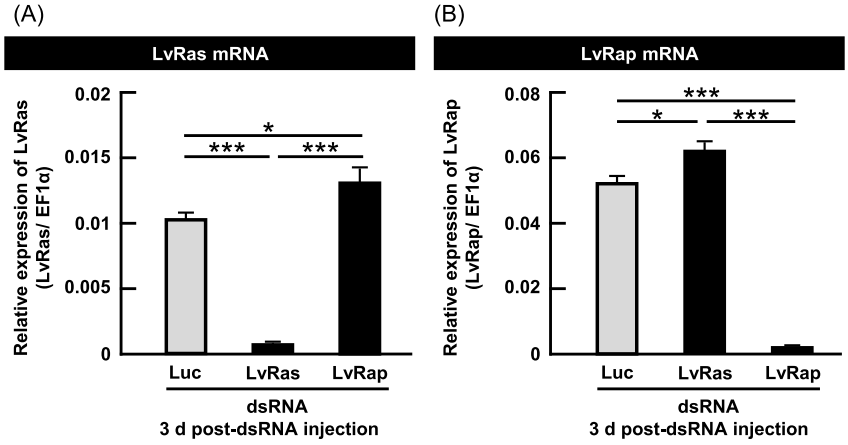

Fig. 7. mRNA expression levels of LvRas and LvRap were reduced *in vivo* after injecting the corresponding dsRNAs. Three days after treatment with the appropriate dsRNA, pooled hemocytes samples (3 shrimp/sample) were collected from each group. *In vivo* gene silencing of LvRas and LvRap was detected by real-time qPCR. Shrimp treated with Luc dsRNA were used as the non-specific dsRNA control group. Asterisks indicate a significant difference between the target mRNA levels and those in the other groups (*$p < 0.05$, **$p < 0.01$).

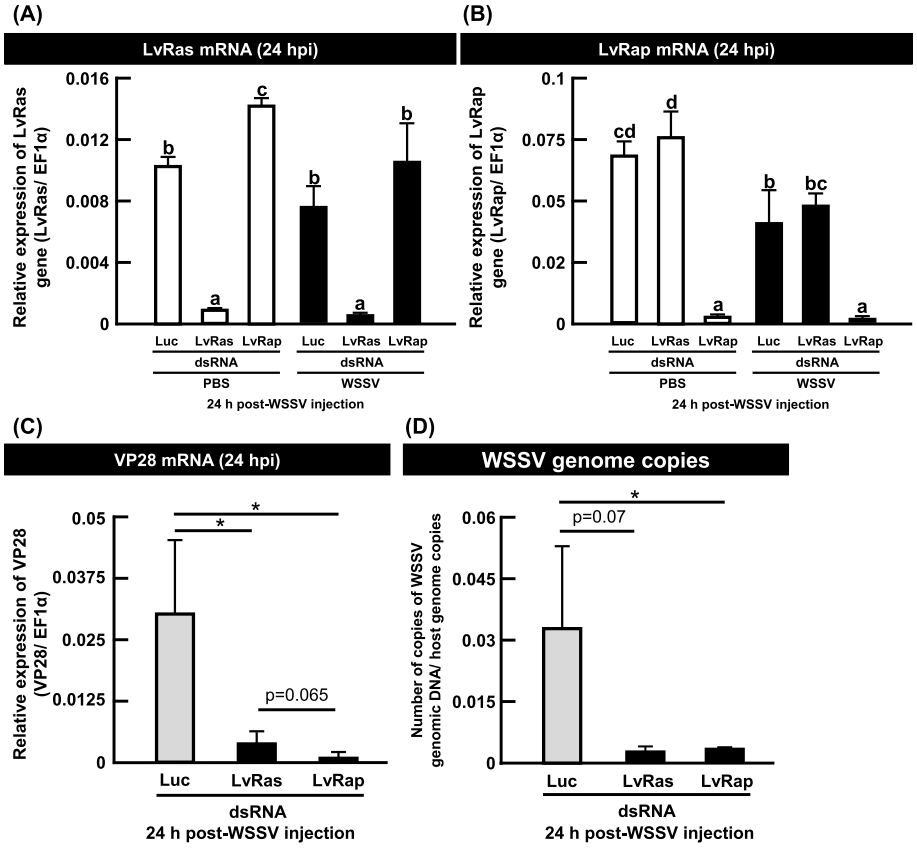

Fig. 8. Gene silencing suggests that LvRas and LvRap are both involved in WSSV replication. Three days after treatment with the LvRas and LvRap dsRNA, shrimp were challenged with WSSV or PBS. At 24 h post challenge, pooled hemocytes and pleopod samples (3 shrimp in each sample) were collected from each group to determine mRNA expression levels and WSSV genome copy numbers, respectively. *In vivo* dsRNA-mediated gene silencing of (A) LvRas and (B) LvRap specifically reduced the mRNA expression level of the target gene. Silencing of either gene also resulted in a decrease of (C)WSSV VP28 gene expression and (D) WSSV genome copy number. Asterisks and bars labeled with different letters represent significantly different values ($p < 0.05$).

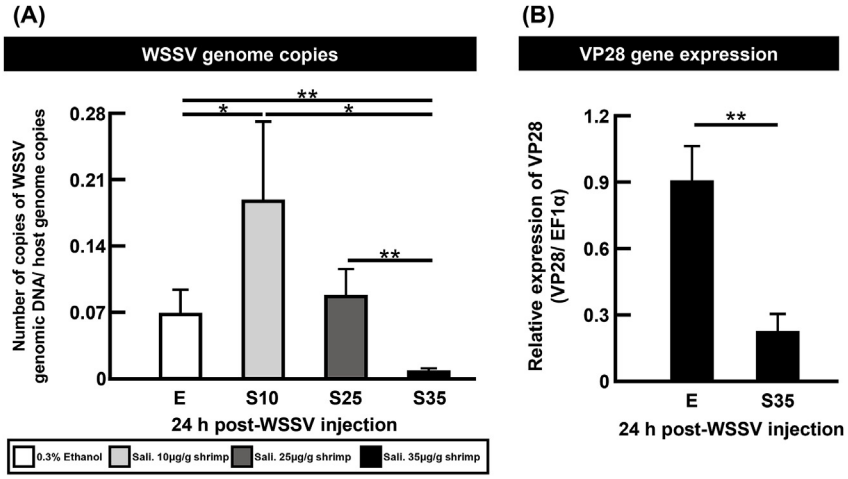

Fig. 9. Treatment with GTP-Ras inhibitor indicates the importance of LvRas activation in WSSV replication. (A) Two hours after treatment with the Ras inhibitor Salirasib at various dosages (10, 25 and 35 μg per g shrimp body weight), shrimp were injected with PBS or WSSV. At 24 h post injection, pooled pleopod samples (3 shrimp per each sample) were collected from each group and the WSSV genome copy number was determined. Shrimp treated with 0.3% ethanol were used as the vehicle control group. In two further experiments with Salirasib at the high dosage (S35) followed by WSSV challenge, (B) pooled hemocytes samples (3 shrimp in each sample) were collected from each group and used to measure WSSV VP28 gene expression and (C) pooled gill samples (6 shrimp in each sample) were collected from each group and used to measure the GTPase activity of LvRas. Asterisks indicate a significant difference between groups (*$p < 0.05$, **$p < 0.01$, ***$p < 0.001$).

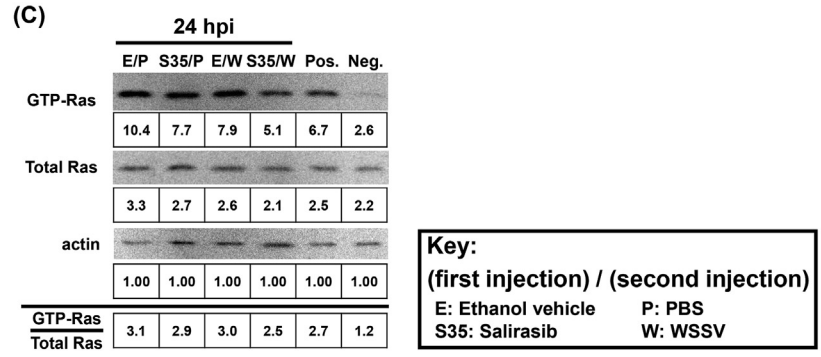

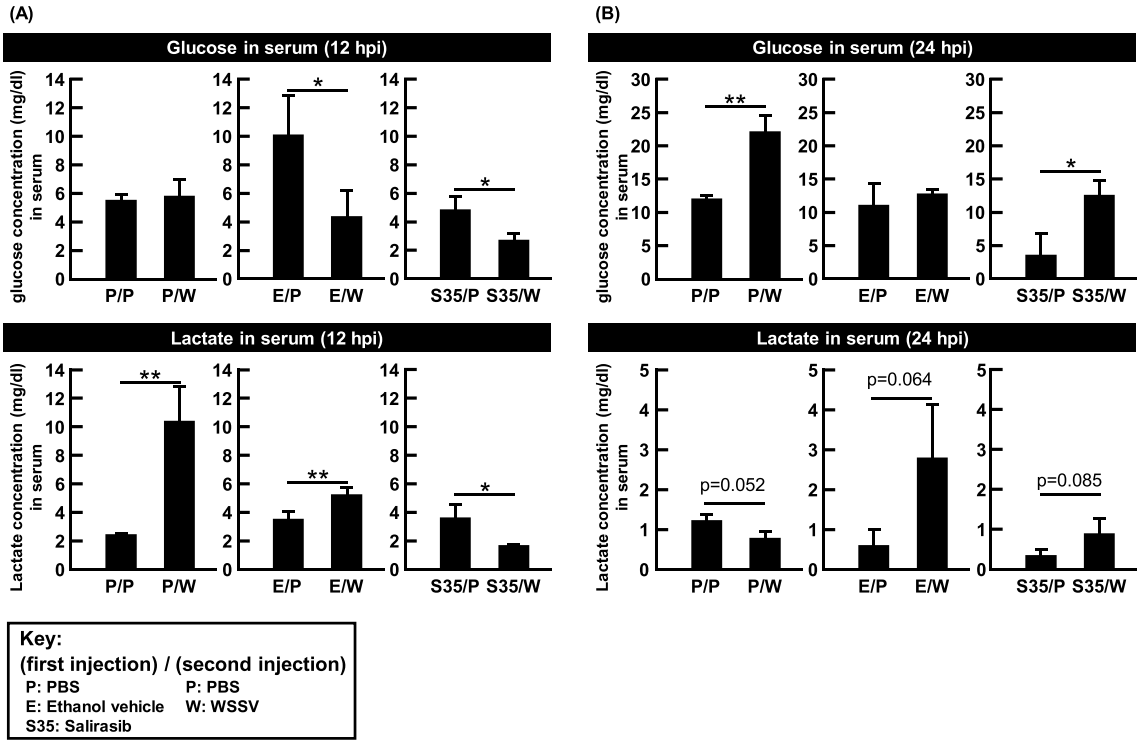

Fig. 10. Lactate accumulation in serum at 12 hpi was no longer seen after pre-treatment with Ras inhibitor Salirasib. Two hours after treatment with Salirasib (35 μg/g shrimp), shrimp were injected with WSSV or PBS. At (A)12 and (B)24 h, pooled hemolymph samples (3 shrimp/sample) were collected and glucose and lactate concentrations were measured. Shrimp treated with 0.3% ethanol were used as the vehicle control group. Asterisks indicate a significant difference between groups (*$p < 0.05$, **$p < 0.01$).

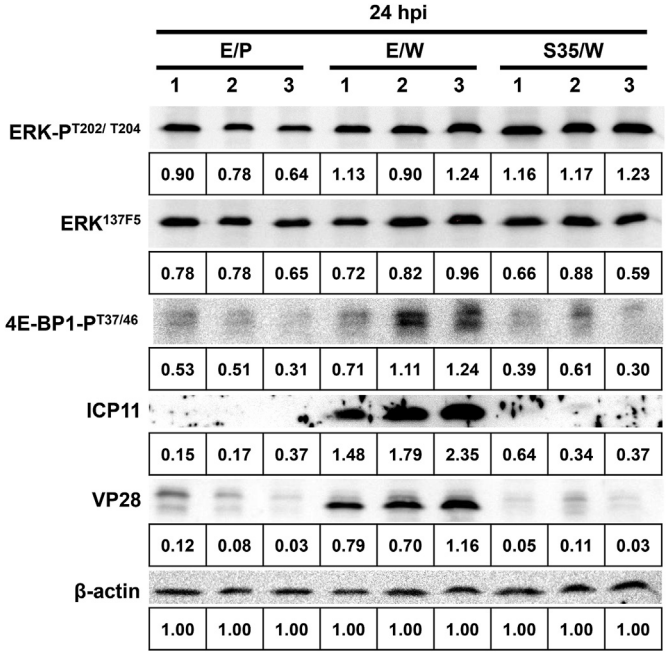

Fig. 11. Effect of Salirasib pretreatment on the activation of the Raf-MEK-ERK and PI3K-Akt-mTOR pathways at the late stage of WSSV infection (24 hpi). Two hours after injection of Salirasib (35 μg/g shrimp), shrimp were injected with WSSV, and 24 h later, pooled gill samples (3 shrimp/sample) were collected. Western blotting was used to detect the expression levels of WSSV proteins and proteins on the ERK and mTOR pathways. Signal levels were quantified using the ImageJ Gel Analysis program and normalized relative to β-actin. E/P: ethanol vehicle/PBS; E/W: ethanol vehicle/WSSV; S35/W: Salirasib/WSSV.

shows that ERK was activated after WSSV infection, while in a previous study, we found that the PI3K-Akt-mTOR pathway was also activated and critical for the WSSV-induced Warburg effect [4]. To evaluate whether LvRas is critical for the activation of these pathways, shrimp were treated with Salirasib before WSSV injection to suppress LvRas activation. Gills were collected from treated shrimps and subjected to western blotting. In results that are consistent with our previous finding in Fig. 9, pretreatment with a high dosage of Salirasib (S35) dramatically reduced the expression levels of two major WSSV late proteins, WSSV VP28 and ICP11, in the WSSV-challenged shrimp (Fig. 11). The suppression of LvRas activation also prevented the WSSV-induced phosphorylation of 4E-BP1, but had no effect on the WSSV-induced levels of phosphorylated ERK. Given that 4E-BP1 phosphorylation indicates activation of the PI3K-Akt-mTOR pathways [4], from these results, we conclude that LvRas activation appears to control the WSSV-induced PI3K-mTOR activation. Meanwhile, although both Figs. 6 and 11 show that the ERK pathway was also activated after WSSV infection, this pathway does not appear to be regulated by LvRas.

4. Discussion

It has already been established that the WSSV-induced Warburg effect (aerobic glycolysis) in shrimp is mediated by the PI3K-Akt-mTOR pathway [4]. In the present paper, our aim was to identify the upstream regulator[s] of this pathway, and since Kras is known to activate PI3K-Akt-mTOR in human cancer cells [50,51], we considered the white shrimp homolog LvRas to be a likely candidate. As shown in Fig. 4, we found that after WSSV infection, mRNA expression of LvRAS was slightly upregulated at both 12 and 24 hpi, and that both the protein expression and the activated GTP-bound form of LvRas were increased at 24 hpi (Figs. 5 and 6). We further showed that suppression of LvRas (and LvRap) mRNA by dsRNA-mediated gene silencing led to a decrease of WSSV VP28 mRNA expression and the number of WSSV genome copies (Fig. 8). Similar effects on WSSV replication and protein

expression were also observed in WSSV-infected shrimp that were pre-treated with the Ras inhibitor Salirasib (Figs. 9 and 11). These data clearly imply that both LvRas and LvRap are important for WSSV pathogenesis. However, previous studies would suggest that regulation of the PI3K-Akt-mTOR pathway is more likely to involve Ras than Rap [52]. Moreover, a specific Rap inhibitor is not available, and since an RNAi silencing platform is unsuitable (our unpublished data suggests that even non-specific dsRNA silencing interferes with the Warburg effect), our next set of experiments focused only on the involvement of LvRas in regulating WSSV-induced aerobic glycolysis via the PI3K-Akt-mTOR pathway.

Fig. 10A shows that at 12 hpi, the Ras inhibitor had no effect on the uptake of glucose in the WSSV-infected shrimp. However, although aerobic glycolysis is one of the hallmarks of the Warburg effect in cancer, we have observed previously (unpublished data) that glucose consumption is not always seen during WSSV infection. Our preliminary data suggests that glutaminolysis may account for this inconsistency, and several recent papers have also suggested that at least in cancer cells, glutaminolysis provides an alternative carbon source for lactate production [53,54]. In any case, Fig. 10a also shows that treatment with the Ras inhibitor caused a significant reduction in the amount of lactate that accumulated in the serum. Further, since phosphorylated 4E-BP1 is an indicator of PI3K-Akt-mTOR activation, the lower level of 4E-BP1-P in the S35/W group in Fig. 11 suggests that Salirasib may have caused the disappearance of WSSV-induced aerobic glycolysis by inactivating the PI3K-Akt-mTOR pathway. By contrast, even though the increased ratio of ERK-P to ERK in WSSV-challenged shrimp (Figs. 6 and 11) implies that WSSV must be activating the Raf-MEK-ERK pathway, we also note that Salirasib treatment had no effect on the levels of activated ERK (Fig. 11). Thus there is no evidence that the activation of this pathway is related to LvRas. From this we conclude that LvRas is not using the Raf-MEK-ERK pathway to regulate the Warburg effect in WSSV-infected shrimp.

Lastly, we note that although we found in multiple repetitions (data not shown) there was only a slight increase in the mRNA levels of LvRas and LvRap at 24 h after viral infection (Fig. 4), there was a significant increase in the levels of Ras protein and activated LvRas (Figs. 5 and 6). This suggests that WSSV infection might primarily affect the activity of Ras at the protein level, and not at the mRNA level. Although this is a phenomenon which has not yet been widely studied, recent reports have shown how a virus might achieve this, for example, via a mechanism known as “shut off” whereby a lytic animal virus selectively inhibits host protein synthesis while increasing the efficiency of virus mRNA translation [55]. Another study used RNA sequencing and ribosome profiling to show that HCMV regulates the translation of cellular mRNAs over the course of infection even as the corresponding transcriptional expression levels remain unchanged [56]. Something similar may be happening in the case of WSSV: taken together Figs. 4–6 and the silencing data suggest that while LvRas expression levels may not need to be upregulated, any reduction in the amount of LvRas protein might result in a significant decrease in virus replication. However, this idea will need to be explored experimentally in a future study.

Acknowledgments

This study was supported financially by the Ministry of Science and Technology (MOST 106-2321-B-006-010, MOST 107-2313-B-006-006-MY3 and MOST 107-3017-F-006-001). We thank Mr. Paul Barlow, National Cheng Kung University, for his helpful criticism of the manuscript.

References

[1] D.V. Lightner, Virus diseases of farmed shrimp in the Western Hemisphere (the Americas): a review, J. Invertebr. Pathol. 106 (2011) 110–130.
[2] P.S. Chang, C.F. Lo, Y.C. Wang, G.H. Kou, Identification of white spot syndrome associated baculovirus (WSBV) target organs in the shrimp *Penaeus monodon* by in situ hybridization, Dis. Aquat. Org. 27 (1996) 131–139.
[3] I.T. Chen, T. Aoki, Y.T. Huang, I. Hirono, T.C. Chen, J.Y. Huang, G.D. Chang, C.F. Lo, H.C. Wang, White spot syndrome virus induces metabolic changes resembling the Warburg effect in shrimp hemocytes in the early stage of infection, J. Virol. 24 (2011) 12919–12928.
[4] M.A. Su, Y.T. Huang, I.T. Chen, D.Y. Lee, Y.C. Hsieh, C.Y. Li, T.H. Ng, S.Y. Liang, S.Y. Lin, S.W. Huang, Y.A. Chiang, H.T. Yu, K.H. Khoo, G.D. Chang, C.F. Lo, H.C. Wang, An invertebrate Warburg effect: a shrimp virus achieves successful replication by altering the host metabolome via the PI3K-Akt-mTOR pathway, PLoS Pathog. 10 (2014) e1004196.
[5] Y.C. Hsieh, Y.M. Chen, C.Y. Li, Y.H. Chang, S.Y. Liang, S.Y. Lin, C.Y. Lin, S.H. Chang, Y.J. Wang, K.H. Khoo, T. Aoki, H.C. Wang, To complete its replication cycle, a shrimp virus changes the population of long chain fatty acids during infection via the PI3K-Akt-mTOR-HIF1α pathway, Dev. Comp. Immunol. 53 (2015) 85–95.
[6] A.E. Karnoub, R.A. Weinberg, Ras oncogenes: split personalities, Nat. Rev. Mol. Cell Biol. 9 (2008) 517–531.
[7] M.C. Mendoza, E.E. Er, J. Blenis, The Ras-ERK and PI3K-mTOR pathways: cross-talk and compensation, Trends Biochem. Sci. 36 (2011) 320–328.
[8] J. Wu, J. Chen, L. Zhang, P.P. Masci, K.N. Zhao, Four major factors regulate phosphatidylinositol 3-kinase signaling pathway in cancers induced by infection of human papillomaviruses, Curr. Med. Chem. 21 (2014) 3057–3069.
[9] M. Martini, M.C. De Santis, L. Braccini, F. Gulluni, E. Hirsch, PI3K/AKT signaling pathway and cancer: an updated review, Ann. Med. 46 (2014) 372–383.
[10] E. Castellano, J. Downward, RAS interaction with PI3K: more than just another effector pathway, Genes Cancer 2 (2011) 261–274.
[11] V. Asati, D.K. Mahapatra, S.K. Bharti, PI3K/Akt/mTOR and Ras/Raf/MEK/ERK signaling pathways inhibitors as anticancer agents: structural and pharmacological perspectives, Eur. J. Med. Chem. 109 (2016) 314–341.
[12] K. Kawada, K. Toda, Y. Sakai, Targeting metabolic reprogramming in KRAS-driven cancers, Int. J. Clin. Oncol. 22 (2017) 651–659.
[13] W. Kolch, Meaningful relationships: the regulation of the Ras/Raf/MEK/ERK pathway by protein interactions, Biochem. J. 351 (2000) 289–305.
[14] Y. Hu, W. Lu, G. Chen, P. Wang, Z. Chen, Y. Zhou, M. Ogasawara, D. Trachootham, L. Feng, H. Pelicano, P.J. Chiao, M.J. Keating, G. Garcia-Manero, P. Huang, K-rasG12V transformation leads to mitochondrial dysfunction and a metabolic switch from oxidative phosphorylation to glycolysis, Cell Res. 22 (2012) 399–412.
[15] D. Gaglio, C.M. Metallo, P.A. Gameiro, K. Hiller, L.S. Danna, C. Balestrieri, L. Alberghina, G. Stephanopoulos, F. Chiaradonna, Oncogenic K-Ras decouples glucose and glutamine metabolism to support cancer cell growth, Mol. Syst. Biol. 7 (2011) 523.
[16] J. Chesney, S. Telang, Regulation of glycolytic and mitochondrial metabolism by ras, Curr. Pharmaceut. Biotechnol. 14 (2013) 251–260.
[17] K.L. Bryant, J.D. Mancias, A.C. Kimmelman, C.J. Der, KRAS: feeding pancreatic cancer proliferation, Trends Biochem. Sci. 39 (2014) 91–100.
[18] R. Courtnay, D.C. Ngo, N. Malik, K. Ververis, S.M. Tortorella, T.C. Karagiannis, Cancer metabolism and the Warburg effect: the role of HIF-1 and PI3K, Mol. Biol. Rep. 42 (2015) 841–851.
[19] J. Son, C.A. Lyssiotis, H. Ying, X. Wang, S. Hua, M. Ligorio, R.M. Perera, C.R. Ferrone, E. Mullarky, N. Shyh-Chang, Y. Kang, J.B. Fleming, N. Bardeesy, J.M. Asara, M.C. Haigis, R.A. DePinho, L.C. Cantley, A.C. Kimmelman, Glutamine supports pancreatic cancer growth through a KRAS-regulated metabolic pathway, Nature 496 (2013) 101–105.
[20] D.R. Wise, C.B. Thompson, Glutamine addiction: a new therapeutic target in cancer, Trends Biochem. Sci. 35 (2010) 427–433.
[21] H. Ying, A.C. Kimmelman, C.A. Lyssiotis, S. Hua, G.C. Chu, E. Fletcher-Sananikone, J.W. Locasale, J. Son, H. Zhang, J.L. Coloff, H. Yan, W. Wang, S. Chen, A. Viale, H. Zheng, J.H. Paik, C. Lim, A.R. Guimaraes, E.S. Martin, J. Chang, A.F. Hezel, S.R. Perry, J. Hu, B. Gan, Y. Xiao, J.M. Asara, R. Weissleder, Y.A. Wang, L. Chin, L.C. Cantley, R.A. DePinho, Oncogenic Kras maintains pancreatic tumors through regulation of anabolic glucose metabolism, Cell 149 (2012) 656–670.
[22] J. Zheng, Energy metabolism of cancer: glycolysis versus oxidative phosphorylation (Review), Oncol Lett 4 (2012) 1151–1157.
[23] Z.Q. Wang, W.T. Cefalu, X.H. Zhang, Y. Yu, J. Qin, L. Son, P.M. Rogers, N. Mashtalir, J.R. Bordelon, J. Ye, N.V. Dhurandhar, Human adenovirus type 36 enhances glucose uptake in diabetic and nondiabetic human skeletal muscle cells independent of insulin signaling, Diabetes 57 (2008) 1805–1813.
[24] D. Vigil, J. Cherfils, K.L. Rossman, C.J. Der, Ras superfamily GEFs and GAPs: validated and tractable targets for cancer therapy? Nat. Rev. Canc. 10 (2010) 842–857.
[25] L. Goitre, E. Trapani, L. Trabalzini, S.F. Retta, The Ras superfamily of small GTPases: the unlocked secrets, Methods Mol. Biol. 1120 (2014) 1–18.
[26] J. Colicelli, Human RAS superfamily proteins and related GTPases, Sci. STKE 2004 (2004) RE13.
[27] R.H. Bender, K.M. Haigis, D.H. Gutmann, Activated K-ras, but not H-ras or N-ras, regulates brain neural stem cell proliferation in a Raf/Rb-dependent manner, Stem Cell. 33 (2015) 1998–2010.
[28] Y.H. Chen, S.M. Gianino, D.H. Gutmann, Neurofibromatosis-1 regulation of neural stem cell proliferation and multilineage differentiation operates through distinct RAS effector pathways, Genes Dev. 29 (2015) 1677–1682.
[29] A. Hennig, R. Markwart, M.A. Esparza-Franco, G. Ladds, I. Rubio, Ras activation revisited: role of GEF and GAP systems, Biol. Chem. 396 (2015) 831–848.
[30] E. Pathak, Analysis of correlated mutations in Ras G-domain, Bioinformation 13 (2017) 174–178.

[31] S. Song, B. Ji, V. Ramachandran, H. Wang, M. Hafley, C. Logsdon, R.S. Bresalier, Overexpressed galectin-3 in pancreatic cancer induces cell proliferation and invasion by binding Ras and activating Ras signaling, PLoS One 7 (2012) e42699.
[32] G.A. Hobbs, C.J. Der, K.L. Rossman, RAS isoforms and mutations in cancer at a glance, J. Cell Sci. 129 (2016) 1287–1892.
[33] A.L. Tetlow, F. Tamanoi, The Ras superfamily G-proteins, Enzymes 33 (2013) 1–14.
[34] B.M. Willumsen, A. Christensen, N.L. Hubbert, A.G. Papageorge, D.R. Lowy, The p21 ras C-terminus is required for transformation and membrane association, Nature 310 (1984) 583–586.
[35] J.F. Hancock, Ras proteins: different signals from different locations, Nat. Rev. Mol. Cell Biol. 4 (2003) 373–384.
[36] I.M. Ahearn, K. Haigis, D. Bar-Sagi, M.R. Philips, Regulating the regulator: post-translational modification of RAS, Nat. Rev. Mol. Cell Biol. 13 (2011) 39–51.
[37] A.D. Cox, S.W. Fesik, A.C. Kimmelman, J. Luo, C.J. Der, Drugging the undruggable RAS: mission possible? Nat. Rev. Drug Discov. 13 (2014) 828–851.
[38] S. Köthe, J.P. Müller, S.A. Böhmer, T. Tschongov, M. Fricke, S. Koch, C. Thiede, R.P. Requardt, I. Rubio, F.D. Böhmer, Features of Ras activation by a mislocalized oncogenic tyrosine kinase: FLT3 ITD signals through K-Ras at the plasma membrane of acute myeloid leukemia cells, J. Cell Sci. 126 (2013) 4746–4755.
[39] B. Rotblat, M. Ehrlich, R. Haklai, Y. Kloog, The Ras inhibitor farnesylthiosalicylic acid (Salirasib) disrupts the spatiotemporal localization of active Ras: a potential treatment for cancer, Methods Enzymol. 439 (2008) 467–489.
[40] T.H. Ng, C.W. Lu, S.S. Lin, C.C. Chang, L.H. Tran, W.C. Chang, C.F. Lo, H.C. Wang, The Rho signalling pathway mediates the pathogenicity of AHPND-causing V. parahaemolyticus in shrimp, Cell Microbiol. 20 (2018) e12849.
[41] H.C. Wang, H.C. Wang, G.H. Kou, C.F. Lo, W.P. Huang, Identification of icp11, the most highly expressed gene of shrimp white spot syndrome virus (WSSV), Dis. Aquat. Org. 74 (2007) 179–189.
[42] A.D. Cox, C.J. Der, M.R. Philips, Targeting RAS membrane association: back to the future for anti-RAS drug discovery? Clin. Cancer Res. 21 (2015) 1819–1827.
[43] O. Warburg, On the origin of cancer cells, Science 123 (1956) 309–314.
[44] J. Lu, M. Tan, Q. Cai, The Warburg effect in tumor progression: mitochondrial oxidative metabolism as an anti-metastasis mechanism, Cancer Lett. 356 (2015) 156–164.
[45] E. Noch, K. Khalili, Oncogenic viruses and tumor glucose metabolism: like kids in a candy store, Mol. Canc. Therapeut. 11 (2012) 14–23.
[46] M.V. Liberti, J.W. Locasale, The Warburg effect: how does it benefit cancer cells? Trends Biochem. Sci. 41 (2016) 211–218.
[47] M.G. Vander Heiden, L.C. Cantley, C.B. Thompson, Understanding the Warburg effect: the metabolic requirements of cell proliferation, Science 324 (2009) 1029–1033.
[48] H. Makinoshima, M. Takita, K. Saruwatari, S. Umemura, Y. Obata, G. Ishii, S. Matsumoto, E. Sugiyama, A. Ochiai, R. Abe, K. Goto, H. Esumi, K. Tsuchihara, Signaling through the phosphatidylinositol 3-kinase (PI3K)/Mammalian target of rapamycin (mTOR) Axis is responsible for aerobic glycolysis mediated by glucose transporter in epidermal growth factor receptor (EGFR)-mutated lung adenocarcinoma, J. Biol. Chem. 290 (2015) 17495–17504.
[49] C. Abildgaard, P. Guldberg, Molecular drivers of cellular metabolic reprogramming in melanoma, Trends Mol. Med. 21 (2015) 164–171.
[50] S. Mabuchi, H. Kuroda, R. Takahashi, T. Sasano, The PI3K/AKT/mTOR pathway as a therapeutic target in ovarian cancer, Gynecol. Oncol. 137 (2015) 173–179.
[51] P. Tomasini, P. Walia, C. Labbe, K. Jao, N.B. Leighl, Targeting the KRAS pathway in non-small cell lung cancer, Oncol. 21 (2016) 1450–1460.
[52] O. Hoeller, P. Bolourani, J. Clark, L.R. Stephens, P.T. Hawkins, O.D. Weiner, G. Weeks, R.R. Kay, Two distinct functions for PI3-kinases in micropinocytosis, J. Cell Sci. 126 (2013) 4296–4307.
[53] F. Hirschhaeuser, U.G. Sattler, W. Mueller-Klieser, Lactate: a metabolic key player in cancer, Cancer Res. 71 (2011) 6921–6925.
[54] I. San-Millán, G.A. Brooks, Reexamining cancer metabolism: lactate production for carcinogenesis could be the purpose and explanation of the Warburg effect, Carcinogenesis 38 (2017) 119–133.
[55] R. Toribio, I. Ventoso, Inhibition of host translation by virus infection in vivo, Proc. Natl. Acad. Sci. U. S. A. 107 (2010) 9837–9842.
[56] O. Tirosh, Y. Cohen, A. Shitrit, O. Shani, V.T. Le-Trilling, M. Trilling, G. Friedlander, M. Tanenbaum, N. Stern-Ginossar, The transcription and translation landscapes during human cytomegalovirus infection reveal novel host-pathogen interactions, PLoS Pathog. 11 (2015) e1005288.